Chapter 2

$Gd_5(Si_xGe_{1-x})_4$ series of alloys

2.1 Discovery of the $Gd_5(Si_xGe_{1-x})_4$ system and the giant MCE

$Gd_5(Si_xGe_{1-x})_4$ alloys were discovered by Holtzberg *et al.* [1] and Smith *et al.* [2]. They found that Gd_5Si_4 orders ferromagnetically at T_C=335 K and that as much as 50% of Ge could be substituted for Si in the silicide structure ($0.5 < x \leq 1$), maintaining the magnetic properties and the orthorhombic structure [1]. Gd_5Ge_4 also had an orthorhombic structure, but different from that of silicide. The germanide structure appeared from x=0 to x=0.25 and presented a strange variety of magnetic phase transitions: a low temperature ordering, which was AFM for Gd_5Ge_4 and FM for the components with added Si, and higher Néel T. Moreover, the paramagnetic Curie temperature (θ_C) yielded a high positive value for all Ge-rich compounds [1]. The intermediate phase was not identified, but since the end members of the solid solution were not isostructural [2, 3] such a discontinuity was to be expected.

In 1997, Pecharsky and Gschneidner discovered a giant magnetocaloric effect in $Gd_5(Si_xGe_{1-x})_4$ alloys [4, 5, 6, 7, 8]. For $Gd_5(Si_2Ge_2)$ [4], the calculation of the magnetic entropy change, ΔS_m, using magnetisation measurements and the Maxwell relation (Eq. 1.6) yielded a value twice larger than that of Gd -the material with the best MCE at room temperature known until then- at~276 K. With the measurements of the heat capacity as a function of T and H, the giant value of ΔS_m was confirmed and the adiabatic temperature change, ΔT_{ad}, as a function of T was evaluated, giving rise to a narrower and higher ($\geq$ 30%) peak than that of pure Gd (see Table 1.1).

In order to understand the unclear magnetic properties and phase relationship in this system, Pecharsky and Gschneidner studied samples in the whole compositon range $0 \leq x \leq 1$, leading to the first phase diagram at zero field of the

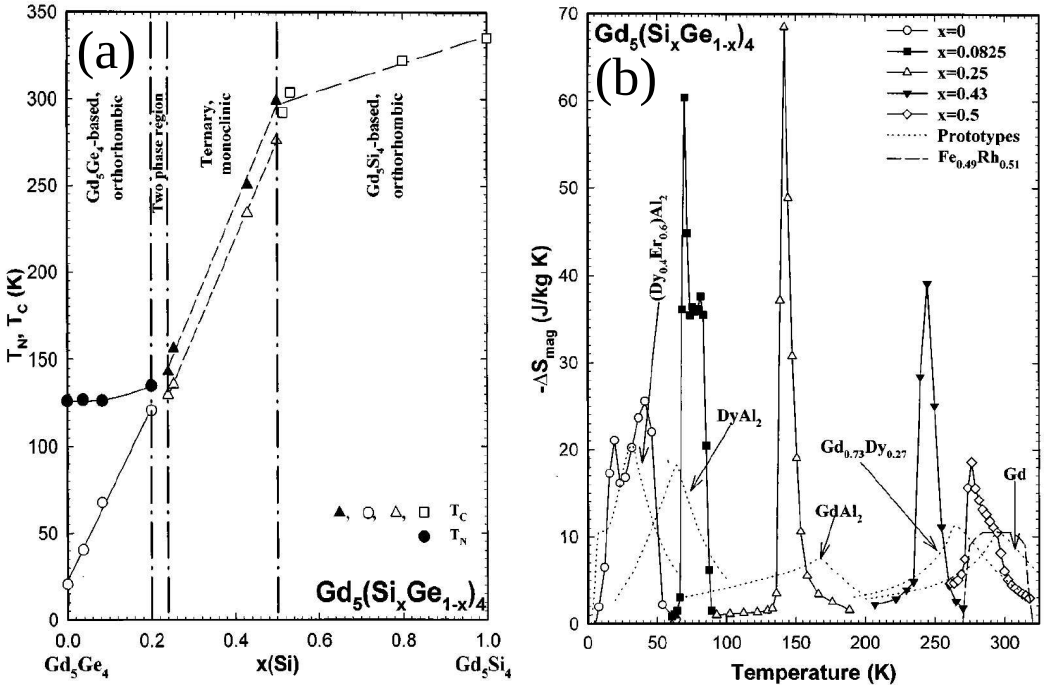

Figure 2.1: (a) First phase diagram at zero field of the $Gd_5(Si_xGe_{1-x})_4$ alloy system, obtained by Pecharsky and Gschneidner [5, 6, 8]. (b)ΔS_m of $Gd_5(Si_xGe_{1-x})_4$ alloys, for $x \leq 0.5$, around their first-order transition, calculated from magnetisation data using the Maxwell relation, for a field variation from 0 to 5 T [5]. ΔS_m values for the best magnetic refrigerant materials are displayed as dotted lines. FeRh is also shown (dashed line) for comparision.

$Gd_5(Si_xGe_{1-x})_4$ system [5, 6, 8] (see Fig. 2.1 (a)). They identified the intermediate phase as monoclinic [6], and showed that the lower transitions in both the Ge-rich region and the intermediate region were first-order and reversible, yielding the giant MCE in these alloys [5]. From x=0 to x=0.2, MCE increased, while it decreased from x=0.24 to x=0.5 [5], being larger than any other prototype material in all temperature ranges (from ~20 K to ~276 K) as shown in Fig. 2.1, (b). In the $0.5 < x \leq 1$ composition region, the PM-FM transition was second-order, leading to a 3 to 3.5-fold reduction of the MCE with respect to that of the compositions showing a first-order transition. These authors were able to increase the transition temperature, T_t, in $Gd_5(Si_2Ge_2)$ from 276 K to 286 K by adding 0.33% at. of Ga, without losing the giant MCE [7].

2.2 Phase diagram of $Gd_5(Si_xGe_{1-x})_4$

The work of Morellon *et al.* [10, 9] unveiled the actual origin of the first-order transition in the two regions where it appears and showed than the upper transition in the intermediate phase does not exist, but it is rather caused by a residual phase with slightly different x [10]. In summary, the phase diagram of the $Gd_5(Si_xGe_{1-x})_4$ alloys at zero field shows three compositional ranges (see Fig. 2.2). The Si-rich compounds ($0.5 < x \leq 1$) display the Gd_5Si_4-type orthorhombic (space group *Pnma*) structure, $O(I)$, with a second order PM-FM transition [5, 6, 8]. For the intermediate region, $0.24 \leq x \leq 0.5$, a first-order magnetostructural phase transition occurs from a high-temperature PM phase (which displays a monoclinic structure, M, space group $P112_1/a$) to a low-temperature FM phase (with the same $O(I)$ structure than the Si-rich compounds), at temperatures ranging linearly from 130 K (x=0.24) to 276 K (x=0.5) [5, 10, 11]. For the Ge-rich compounds ($x \leq 0.2$), a second-order PM-AFM transition occurs at T_N (from ~125 K for x=0 to ~135 K for x=0.2) [5]. Upon further cooling, a first-order AFM-FM transition takes place, whose temperature ranges linearly from about 20 K (x=0) to 120 K (x=0.2). Because of its singularity, the case x=0 is discussed in section 2.4.1. Since neutron scattering cannot be performed in Gd-based compounds, the nature of the AFM phase is currently under discussion [9]: the magnetic structure might correspond to that of either a canted ferrimagnet, as proposed for Nd_5Ge_4 [12] or a canted antiferromagnet, as for the Ge-rich region of the $Tb_5(Si_xGe_{1-x})_4$ alloys [13, 14]. The AFM-FM transition occurs simultaneously with a first-order structural transition from a high-temperature Sm_5Ge_4-type orthorhombic (space group *Pnma*) phase, $O(II)$, to the low-temperature $O(I)$ phase [9]. We must note that in this case the symmetry remains unchanged through the transition, although drastic variations in the cell parameters and atomic positions also occur (see section 2.3). In the range $0.2 < x < 0.24$, where the second-

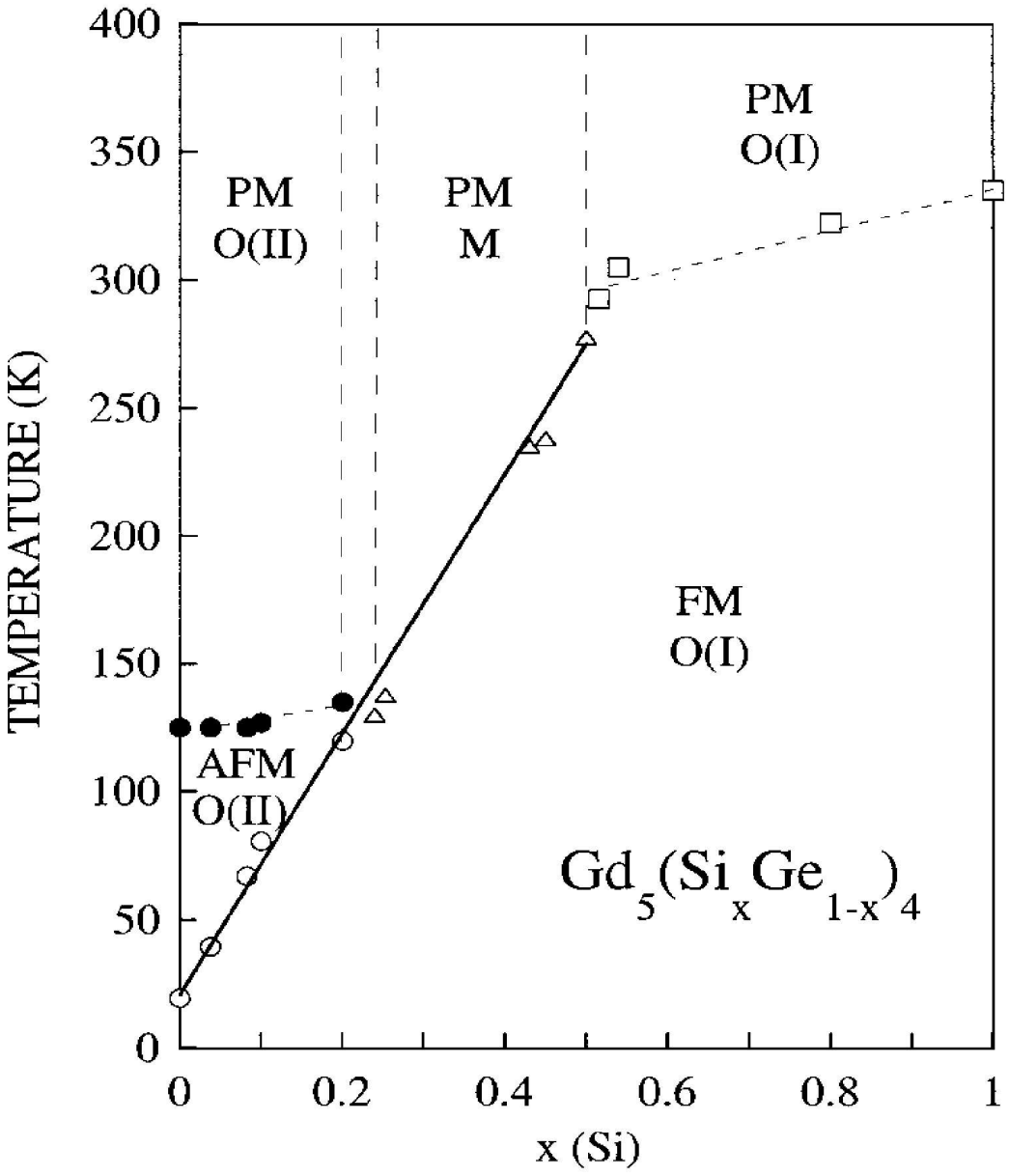

Figure 2.2: Magnetic and crystallographic phase diagram at zero field, for $Gd_5(Si_xGe_{1-x})_4$ alloys, as a function of temperature and composition [9]. PM stands for paramagnetic phase, FM for ferromagnetic phase and AFM for antiferromagnetic phase. M stands for monoclinic structure, O(I) for Gd_5Si_4-type orthorhombic structure and O(II) for Gd_5Ge_4-type orthorhombic structure. First-order transition is displayed as a solid line.

order PM-AFM transition disappears, $O(II)$ and M structures coexist [6]. In both the Ge-rich and intermediate compositional region, the first-order transition may be induced reversibly by an applied magnetic field [5, 10, 9] and by an external hydrostatic pressure [10, 15, 16], which both linearly shift T_t up to higher temperatures. The fact that the transition may be field-induced gives rise to very exciting and novel properties (see below).

A phenomenological description of the first-order magnetostructural transition given in Ref. [17] derive the $H - T$ magnetic phase diagram and accounts for the thermal and magnetic hysteresis occurring in these alloys.

There are some other details in the phase diagram for $Gd_5(Si_xGe_{1-x})_4$ alloys that make it much more complex. Different heat treatments of the samples and the purity of the components may lead to the stabilisation of different crystallographic structures, which also influence the magnitude of the MCE [18], specially in the boundaries of the compositional regions. Pecharsky *et al.* [19] published a phase diagram with some differences with respect to that in Fig. 2.2, using alloys with high-purity Gd. The same authors found a new transition in the compounds around $x \cong 0.5$ [18, 20, 21]. It is an irreversible transition occurring between ~500 K and ~870 K, from the room-temperature M phase, that yields the $O(I)$ phase again. Then, after cooling down to room temperature again, the compound behaves like the Si-rich alloys (with the second-order PM-FM transition without structural transformation). If the compound is further heated up to ~1070-1570 K [18, 20, 21], the M structure reforms, returning to the behaviour of the intermediate-region compounds. Accordingly, a reversible $M \leftrightarrow O(I)$ transition -not directly observed- exists between ~870 K and ~1070 K.

2.3 Microstructure and atomic bonds

In order to understand the singular behaviour of these alloys [5, 6, 10, 9], the atomic structure has been analysed in detail in literature. The transition is presently understood by considering the layered crystal structure of $Gd_5(Si_xGe_{1-x})_4$ [22]. Gd atoms (represented as blue spheres in Fig. 2.3; vertex of polyhedra also represent Gd positions) form a two-dimensional (3^2434) net (Figure 2.3 (a)). This quasi-infinite layer (slab) is composed of distorted cubes and trigonal prisms which share common faces. T atoms, which are a mixture of Si and Ge atoms (green spheres in Fig. 2.3), occupy the trigonal prisms, sharing a common rectangular face to produce a T-T dimer (intraslab bond). The Gd atom at the center of each cube is surrounded by 4 T and 2 T' atoms (red spheres) [23]. For x=0.5 compound, the occupancy in T atoms is 60% Ge and 40% Si, being 60% Si and 40% Ge for T' atoms [23]. The T' atoms play a key role in the interslab bonding thus controlling both the crystal structure and properties of the alloys. For the

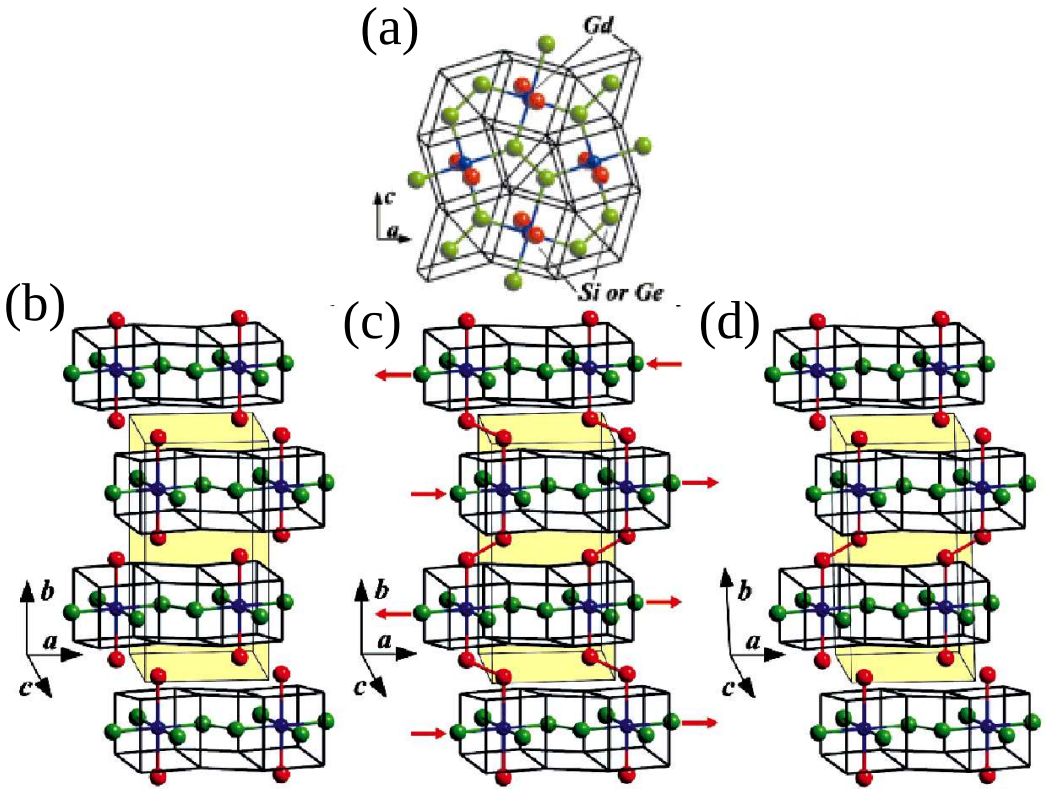

Figure 2.3: Crystallographic structures of $Gd_5(Si_xGe_{1-x})_4$ alloys. (a) Projection along **b** axis, which is common for all structures and emphasise the basic building slabs (3^2434 net), with Gd atom (in blue) inside the cubes and T atoms (mixture of Si and Ge, in green) inside the trigonal prisms. (b) Sm_5Ge_4-type orthorhombic structure [$O(II)$]. (c) Gd_5Si_4-type orthorhombic structure [$O(I)$]. (d) Monoclinic structure (M). The projection along **c** axis emphasises T' atoms (mixture of Si and Ge, in red) and the covalent-like bonds between slabs. Note that one half of the bonds are broken in the M phase, while all of them are broken in the $O(II)$ phase. Red arrows indicate the shear displacement of the slabs in the $O(I)$ phase when the transition to the two other possible phases occurs.

$O(I)$ phase (Fig. 2.3 (c)), which is always FM, two-dimensional slabs (layers) are connected one another through T'-T' covalent-like bonds [22, 23]. The interslab bonds are totally broken when the distance between all T' atoms increases during the transformation to the $O(II)$ phase [9, 22] (Fig. 2.3 (b)), yielding an AFM phase, while only half of the T'-T' bonds are broken during the transformation to the M phase [22, 23] for $0.24 \leq x \leq 0.5$ compounds (Fig. 2.3 (d)), leading to a PM phase. The breaking of the bonds, *i.e.* the structural transition, occurs by a shear mechanism (also depicted in Fig. 2.3) along the **a** axis [23] in both composition regions (the distance between T' atoms expands by 32.7% in the intermediate compounds ($0.24 \leq x \leq 0.5$) [23] and by 34% in the Ge-rich compounds ($x \leq 0.2$) [9]), and yields a large volume variation (~0.4% and ~0.5%, respectively). To illustrate this fact, Fig. 2.4 shows the variation of the lattice parameters and the distance between T' atoms when the $O(I) \leftrightarrow O(II)$ transition is thermally induced in x=0.1 compound. The three structures ($O(I)$, M and $O(II)$) are thus present at room temperature by tunning the Si:Ge ratio (x) from Gd_5Si_4 to Gd_5Ge_4. Figure 2.5 (a) displays the values of the lattice parameters for the whole compositional range at room temperature. The shifts in all atomic positions between the three crystal structures are depicted in Fig. 2.5 (b). As mentioned above, the main difference between the structures is the shift of the atomic positions along the **a** axis, especially affecting the distance between T' sites.

2.4 Structural and magnetic properties

Crystallography and magnetism are closely related in $Gd_5(Si_xGe_{1-x})_4$ [22, 23, 24, 25, 26]. On one hand, Choe *et al.* [23] investigated this relationship by calculating the efective exchange parameter $J(\mathbf{R})$ between Gd sites in the different phases present in $Gd_5(Si_2Ge_2)$, where **R** is the Gd-Gd distance (see Fig. 2.6). They used a nearly free electron model for the conduction band and applied the Ruderman-Kittel-Kasuya-Yosida (RKKY) model. It was found that in the M phase, $J(\mathbf{R})>0$ for short Gd-Gd contacts and $J(\mathbf{R})<0$ for long Gd-Gd contacts, while in the $O(I)$ phase $J(\mathbf{R})>0$ for the entire range of Gd-Gd interactions. An hypothetical $O(II)$ phase in $Gd_5(Si_2Ge_2)$ would lead to $J(\mathbf{R})<0$ for the whole range of **R**. Therefore, the significant changes in electronic structure when the crystal structure varies affect the exchange interactions, and the values of $J(\mathbf{R})$ may account for the change in the magnetic behaviour of the various crystal structures.

On the other hand, it is worth noting that ferromagnetism only exists in the $O(I)$ structure, *i.e.* as long as all slabs are connected by T'-T' covalent-like bonds [22]. In order to explain this fact, Levin *et al.* [24] proposed that ferromagnetism in the $O(I)$ ground state is achieved not only via the indirect RKKY $4f-4f$ exchange, but also via a direct Gd-Ge(Si)-Gd superexchange through the interslab

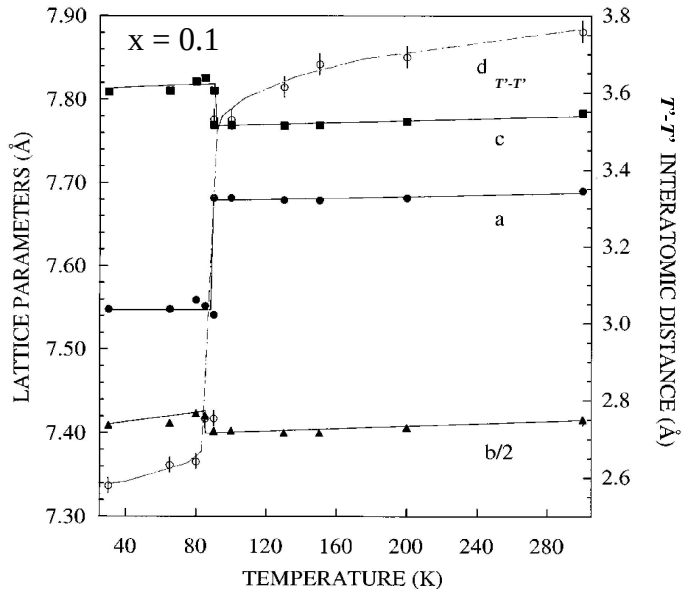

Figure 2.4: Thermal dependence of the lattice parameters (solid symbols) and $T' - T'$ interatomic distance (open symbol) of $Gd_5(Si_xGe_{1-x})_4$ for x=0.1, obtained from XRD. The transition $O(I) \leftrightarrow O(II)$ is clearly observed at T_t=81 K. The lines are a guide to the eye. Taken from Ref. [9].

covalent-like bonds. It is well-known that the indirect RKKY exchange between $4f - 4f$ localised electrons, through the $6s$ itinerant electrons, accounts for most of the phenomenology in lanthanide systems. But in the present system, although RKKY is certainly important, it does not account for the abrupt change in magnetic behaviour (PM↔FM) at the crystallographic transition. Even though there would be a relevant change in the RKKY interaction along the **a** axis (where there is the shear displacement that leads to the 0.8 to 1.1 Å increase of T'-T' distances [10, 22, 23]), the change in the distances along the **b** and **c** axes is fairly smaller. Therefore, the overall RKKY interaction is expected to have a minimal variation. However, if in addition to the RKKY interaction, there were a Gd-Si(Ge)-Gd superexchange interaction in the low-temperature FM $O(I)$ phase propagating through the interslab covalent-like bonds, then the breaking of all (or half) of them at the structural transformation would explain the destruction of the ferromagnetism in the system, since the superexchange interaction should disappear. This suggestion is supported by the fact that T_C in the Si-rich compounds ($0.5 < x \leq 1$), which always have the $O(I)$ structure, is higher than that of pure Gd (by as much as ~40 K) [1, 5]. Accordingly, the magnetic behavior of the $Gd_5(Si_xGe_{1-x})_4$ compounds can be understood qualitatively in terms of competition between intraslabs (conventional indirect $4f - 4f$ RKKY) and interslab

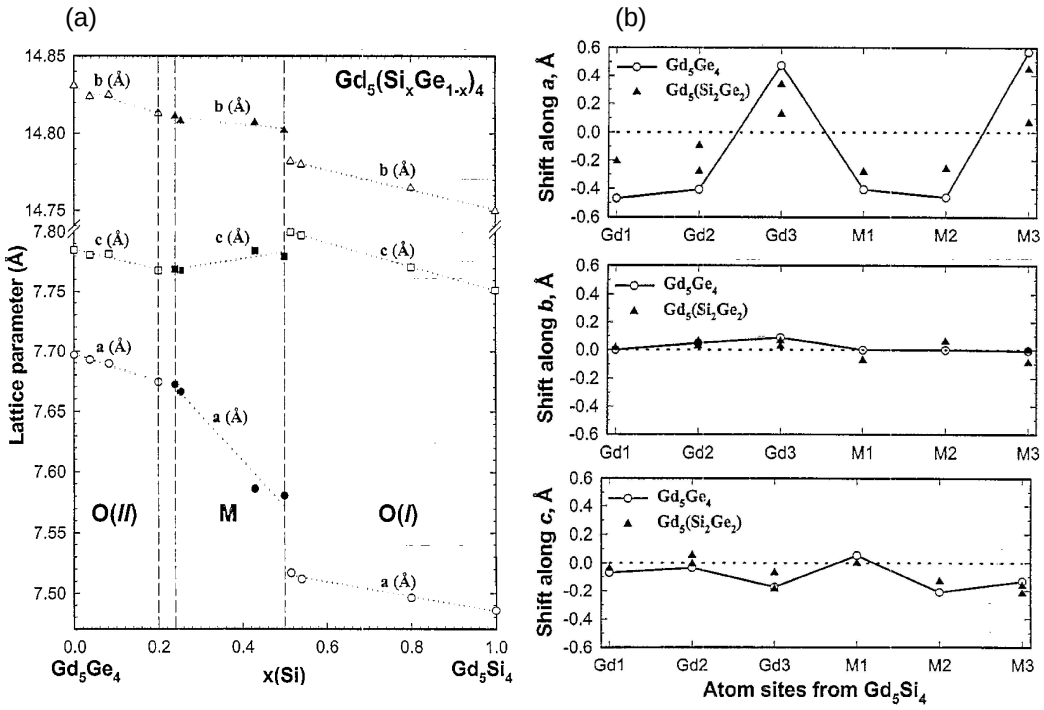

Figure 2.5: (a) Lattice parameters for the $Gd_5(Si_xGe_{1-x})_4$ system at room temperature. The dotted lines are a guide to the eye. The dashed lines delineate structural phase regions. (b) Relative atomic shifts along **a**, **b**, and **c** axes, in the crystal structures of Gd_5Ge_4 [$O(II)$] and $Gd_5(Si_2Ge_2)$ (M), with respect the positions in Gd_5Si_4 [$O(I)$]. M1 and M2 are T-type atoms, while M3 is T'-type atom. Taken from Ref. [6].

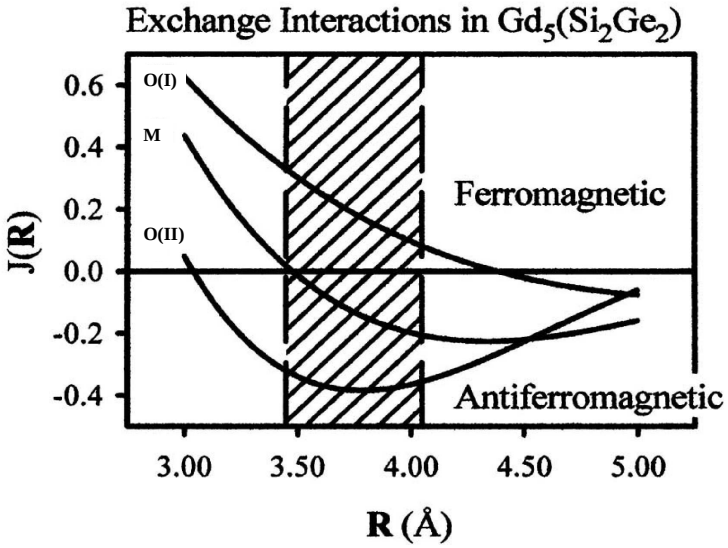

Figure 2.6: Variations in the exchange interactions, $J(\mathbf{R})$, between Gd atoms in $Gd_5(Si_2Ge_2)$ with Gd-Gd distance, **R**, as estimated from the RKKY model using a nearly free electron model for the conduction electrons. The hatched region between 3.45 and 4.05 Å corresponds to the range of short Gd-Gd distances. Taken from Ref. [23].

exchange interactions (Gd-Ge(Si)-Gd superexchange propagated via the covalent-like bonds) [15, 22, 24].

Rao also discussed possible correlations between crystal structure and magnetism [25]. The author established an almost linear dependence between T_C and the lenght of T'-T' bonds, for the whole compositional range ($0 \leq x \leq 1$). The lenght of the bonds is thus a crucial structural parameter governing the magnetic interactions in these compounds. It is also suggested that FM interactions stabilise the $O(I)$ phase at low temperature in the intermediate region. Moreover, Liu *et al.* [26] demonstrated that the $Gd_5(Si_xGe_{1-x})_4$ compounds form a completely miscible solid-solution crystallised in the $O(I)$ structure at low temperature. This feature is interpretated by considering the competing effects of lattice strain (induced by the substitution of Ge for Si) and ferromagnetic exchange interactions, which thus help to stabilise the $O(I)$ phase for $x \leq 0.5$ below T_C.

This strong coupling between the magnetic and crystallographic sublattices enables the existence of a field-induced order-disorder phase transition (PM-FM in the $0.24 \leq x \leq 0.5$ range), which is rarely observed. Only MnAs-based alloys [27, 28, 29], $La(Fe_xSi_{1-x})_{13}$ compounds [30, 31] and the manganite $Sm_{0.65}Sr_{0.35}MnO_3$ [32] are some of the few cases. In $0.24 \leq x \leq 0.5$ compounds both crystallographic phases coexist during the first-order phase transition, therefore a coexis-

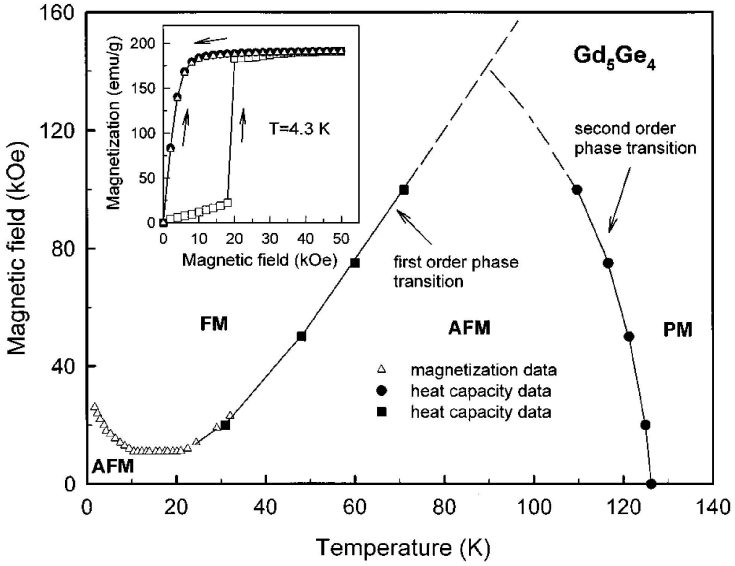

Figure 2.7: The magnetic phase diagram of Gd_5Ge_4 obtained from the heat capacity and magnetisation data. The AFM→FM transition within ~1.8 and ~25 K is completely or partially irreversible (see text for details). The inset shows the magnetisation of Gd_5Ge_4 cooled in zero magnetic field. During the first magnetic field increase, which is shown by open squares in the inset, a metamagnetic-like transition occurs at ~18 kOe. During the first magnetic-field reduction (closed circles) and during the second and following magnetic-field increases (opened triangles), the magnetisation behaviour is typical of a soft ferromagnet. Taken from Ref. [35].

tence of ordered (FM) and disordered (PM) magnetic phases is observed [24, 33].

Finally, concerning the anisotropy of the magnetic properties, a study in a $x \cong 0.5$ single crystal along the three crystallographic directions shows a small anisotropy in magnetisation, which is thus also observed in MCE [34].

2.4.1 The x=0 case

The magnetic ground state of the Gd_5Ge_4 alloy had been reported to be that of a simple AFM with T_N ~15 K [1], but recent works clearly show that Gd_5Ge_4 orders AFM at T_N ~127 K, and that no FM phase is observed when cooling at zero field down to ~1.8 K, the crystallographic structure remaining at the $O(II)$ phase [35, 36, 37, 38]. This fact is in disagreement with the behaviour of the Ge-rich compounds ($0<x\leq0.2$), which order AFM at ~125-135 K and upon further cooling undergo a first-order AFM/$O(II)$-to-FM/$O(I)$ transition (see sec. 2.2). However, for x=0, the application of a field of 18 kOe (H_{cr}) at 4.3 K irreversibly

transforms the AFM state into a FM state, with also an irreversible $O(II) \rightarrow O(I)$ transition, since after the field is reduced isothermally back to zero, Gd_5Ge_4 still remains in the FM/$O(I)$ state. The inverse FM/$O(I)$→AFM/$O(II)$ transition can be induced by heating the sample to above ~25 K, where the well-known first-order reversible transition occurs, in concordance with the rest of Ge-rich alloys. From 4.3 to ~10 K, H_{cr} decreases with temperature, while from ~10 K to ~20 K becomes nearly constant (~11 kOe). The latter temperature range shows a more complex behaviour, because the transition in this case is partially reversible. Above ~25 K, the transition is completely reversible and shifts linearly with the magnetic field [35, 36, 37, 38]. The same overall behaviour is observed when the first-order AFM/$O(II)$→FM/$O(I)$ is induced by external hydrostatic pressure instead of magnetic field [15]. The magnetic phase diagram for x=0 is displayed in Fig. 2.7.

The antiferromagnetism related to the $O(II)$ phase is believed to be similar to that of the Ge-rich $Tb_5(Si_xGe_{1-x})_4$ alloys, which have the same structural phase. In the ordered phase of Tb_5Ge_4, the individual slabs have canted 2D ferromagnetism while the interslab ordering is canted antiferromagnetic, leading to 3D ordering [13, 14]. A spin reorientation occurs with T in the AFM state, affecting the intraslab ferromagnetic canting, but the state remains AFM [14]. In contrast, the ground state of Tb_5Si_4 is canted FM, with also a spin reorientation occuring with T [14]. Figure 2.8 shows the magnetic structures present in Tb_5Ge_4 and Tb_5Si_4 compounds. In the case of the AFM phase in Gd_5Ge_4, the extrapolated Curie-Weiss temperature is positive [1, 8, 36, 39], which is an evidence of the existence of positive (FM) exchange interactions in the AFM phase and it is thus reasonably to compare both materials. Magen *et al.* [15] proposed for Gd_5Ge_4 a model of magnetic interactions similar to Tb_5Ge_4, shown in Fig. 2.9. For Levin *et al.* [36], the anisotropy in the exchange interactions of Gd atoms may account for the difference between the interslab (AFM) and intraslab (FM) magnetic ordering and therefore for the variety of probably non-colinear magnetic structures present in Gd_5Ge_4. Szade *et al.* [39] studied the inverse of the low-field magnetic susceptibility in Gd_5Ge_4 at high temperature and detected a non-linear behaviour between T_N and ~230 K, indicating the onset of some ordering process.

2.5 Other properties

The field-induced, reversible nature of the first-order magnetostructural transition in $Gd_5(Si_xGe_{1-x})_4$ alloys for $x \leq 0.5$, results in colossal magnetostriction [10, 9, 11, 37], giant magnetoresistance [40, 41, 42, 43], unusual Hall effect [44], and spontaneous generation of voltage [45, 46], besides the giant MCE. Some of the most relevant of these properties are explained briefly.

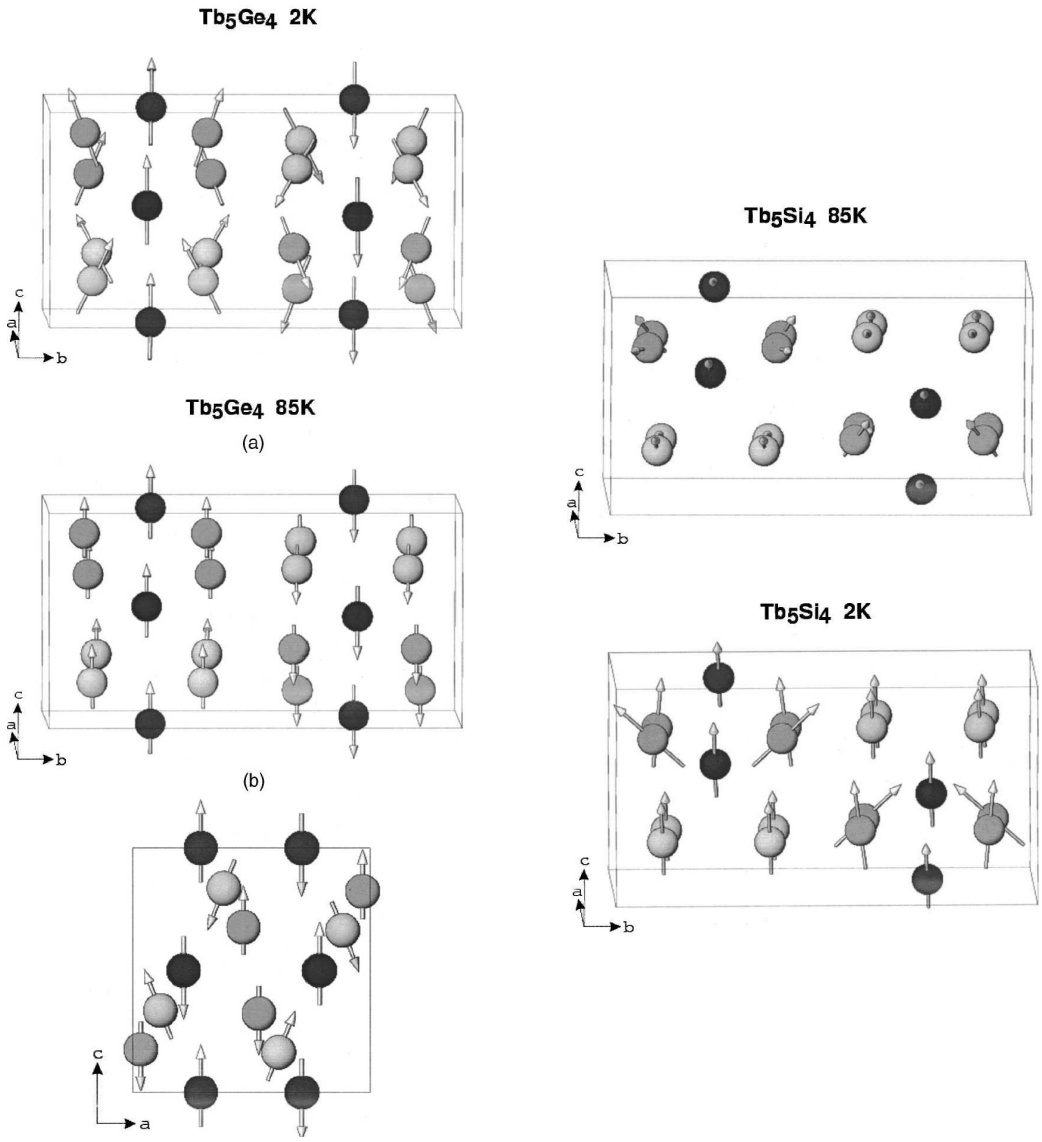

Figure 2.8: Magnetic structures of Tb_5Ge_4 and Tb_5Si_4 at 2 K and 85 K as determined from neutron powder diffraction data, showing the two distinct phases that each compound shows at low temperatures. The spheres stand for Tb ions, and a different level of shading is used to identify Tb1 (black), Tb2 (medium gray), and Tb3 (lightest gray). For Tb_5Ge_4 at 85 K, the projection in the **a**-**c** plane has been included to emphasise the canting of the Tb3 ions. Taken from Ref. [14].

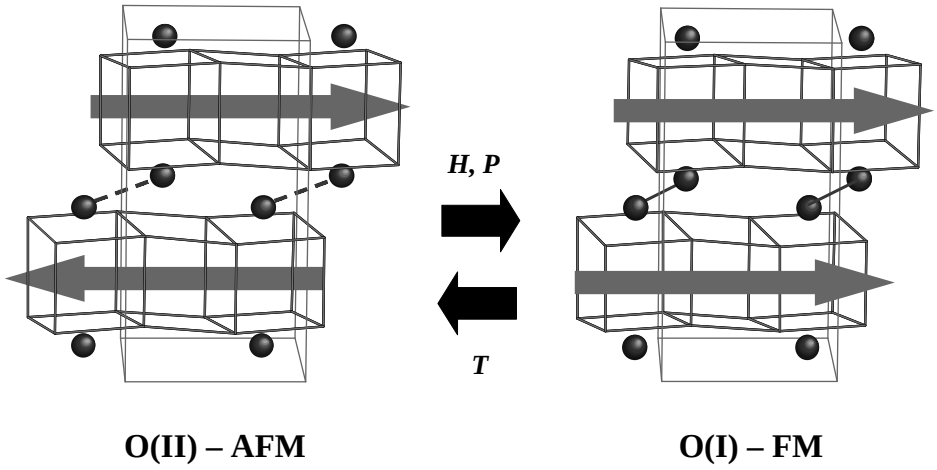

Figure 2.9: Crystallographic and magnetic structures of Gd_5Ge_4 in the **a**-**b** plane at low temperature. Only the Ge atoms participating in the T'-T' covalent-like bonds are depicted as solid spheres. Solid lines stand for formed bonds while dashed lines represent broken bonds. Gray arrows are used to illustrate the change in the magnetic coupling induced by field, hydrostatic pressure or temperature. Taken from Ref. [15].

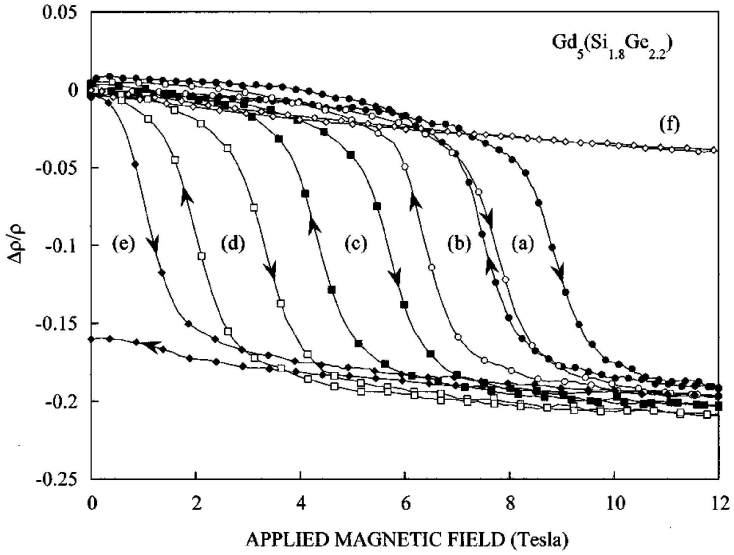

Figure 2.10: Magnetoresistance ratio $\Delta\rho/\rho = [\rho(H,T) - \rho(0,T)]/\rho(0,T)$ for the $Gd_5(Si_xGe_{1-x})_4$ compound with x=0.45 as a function of the applied magnetic field at some selected temperatures of (a) 275, (b) 270, (c) 260, (d) 250, (e) 240, and (f) 230 K. Taken from Ref. [40].

2.5.1 Giant magnetorresistance

A remarkable phenomenology in $Gd_5(Si_xGe_{1-x})_4$ is that of the magnetoresistance, because it also shows a giant effect -giant magnetoresistance (GMR)-, both in $0.24 \leq x \leq 0.5$ compounds [40, 41, 42], see for example Fig. 2.10, and in the $0 \leq x \leq 0.2$ alloys [43]. Since the two structural phases involved in the transition show a different electrical resistance, which at T_t is ~20-25% for $0.24 \leq x \leq 0.5$ and ~50% for $0 \leq x \leq 0.2$, a drastic change in the resistance leads to a GMR ~20-50% when the transition to the low-temperature $O(I)$ phase is field-induced above T_t. The application of a field at the $O(I)$/FM phase yields a negative but small magnetoresistance, corresponding to a FM system with localised moments [40].

The study of GMR in this series of alloys has unveiled that the electrical resistance of the high-temperature phase (M or $O(II)$, depending on the compositional region) changes when the material is cycled through the structural transition [47, 48]. For clarity, we will call the low-temperature $O(I)$ phase α, while we will call the high-temperature phase β' or β" depending o the resistance value. For a virgin sample, the low-temperature α phase shows a higher resistance than high-temperature β' phase (giving rise to a positive GMR). But when the sample is thermally cycled through the first-order phase transition, a high-temperature β"

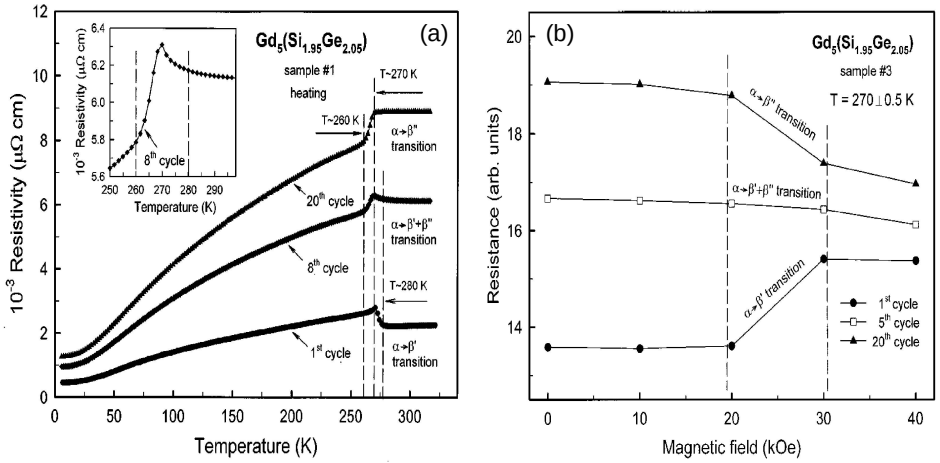

Figure 2.11: (a) Temperature dependences of the electrical resistivity of $Gd_5(Si_xGe_{1-x})_4$ compound with x=0.4875 on heating in zero field during the 1st, 8th, and 20th cycle through the first-order phase transition. The inset shows the detailed behaviour between 250 and 300 K during the 8th cycle. (b) Magnetic field dependences of the electrical resistance of the same compound measured under increasing field after a different number of isothermal cycles through the first-order phase transition at 270 K. Taken from Ref. [47].

phase with higher resistance than α phase is obtained (giving rise now to a negative GMR), see Fig. 2.11 (a). The same phenomenon occurs when the sample is cycled through the transition by the application of a magnetic field, as show in Fig. 2.11 (b). Moreover, it is also observed that T_t of the $\alpha \leftrightarrow \beta$" transition is lower by ~2-7 K than that of $\alpha \leftrightarrow \beta$'. The effect is suggested to be originated from a redistribution of the Si/Ge ratio in T and T' atoms [47]: Si content increases in the intraslab positions (T) and decreases in the interslab positions (T', where the covalent-like bonds between slabs take place). The structural transition occurs at lower T_t because Ge-rich T'-T' bonds are weaker, as derived from the phase diagram (T_t decreases by ~11 K for each 1 at. % increase in Ge content in the bulk alloy, see Fig. 2.2). The difference between the behaviour of the resistance during the $\alpha \leftrightarrow \beta$' and $\alpha \leftrightarrow \beta$" transitions is settled by two main contributions that arise from the change in the conduction electron concentration and scattering processes during the first-order phase transition. Another fact observed in resistance studies is that the residual resistivity increases at each cycle due to the increasing precence of microcracks [40, 41, 42, 47]. This suggests that the large volume change taking place at the first-order transition damages irreversibly these samples by introducing stress at the grain boundaries.

The electrical resistance also shows an anomalous behaviour in the second-order AFM-FM transition (for $0 \leq x \leq 0.2$ compounds). In this case, the resistance changes from a metallic behaviour in the FM phase (resistance increases with T) to a semiconductor-like behaviour (resistance smoothly decreases with T) [35, 39, 43, 48].

2.5.2 Colossal magnetostriction

The change in the crystal structure at T_t leads to a huge linear thermal expansion (LTE) of $\Delta l/l \cong 0.16\%$ for $0 \leq x \leq 0.2$ (*i.e.*, a volume change $\Delta V/V = 3(\Delta l/l) \cong 0.48\%$) [9, 37] and $\Delta l/l \cong 0.13\%$ ($\Delta V/V \cong 0.4\%$) for $0.24 \leq x \leq 0.5$ [10], see for example the inset in Fig. 2.12 for x=0.1. The purity of Gd in the samples affects the value of the LTE (and therefore the volume expansion) at the first-order transition [49]. LTE measurements carried out in a single crystal with x=0.43 showed that $\Delta l/l$ are negative along the **b** and **c** axes (-0.20% and -0.21%, respectively), while it is positive along the **a** axis (+0.68%), leading to a volume change of ~0.27% [11]. Similar results were obtained by Han *et al.* with a $x \cong 0.5$ single crystal [50], who also measured LTE along the **a** axis as a function of the angle of the applied field [51]. Since the transition is field-induced, a strong magnetostriction is expected at temperatures above T_t, for the corresponding transition field. The magnetostriction measurements are independent of the field direction in polycrystalline samples ($\lambda_{\parallel} = \lambda_{\perp}$), and consequently the volume magnetostriction may be evaluated as $\omega = 3\lambda_{\parallel(\perp)}$. For $0 \leq x \leq 0.2$ alloys, a large value of the volume magnetostriction $\omega \cong 0.5\%$ is reached [9, 37] (Fig. 2.12 for x=0.1), while for $0.24 \leq x \leq 0.5$ alloys, $\omega \cong 0.45\%$ [10]. Accordingly, $Gd_5(Si_xGe_{1-x})_4$ compounds for $x \leq 0.5$ are potential candidates as magnetostrictive transducers.

2.6 Characterisation of $Gd_5(Si_xGe_{1-x})_4$ alloys

2.6.1 Electronic structure

The knowledge of the electronic structure of $Gd_5(Si_xGe_{1-x})_4$ alloys is relevant in order to understand the properties of these compounds. The electronic structure has been experimentally investigated by X-ray and ultraviolet photoelectron spectroscopy (XPS and UPS) on the valence band [39, 52]. Covalent bonding between Gd and Si or Ge causes a charge redistribution which is observed to be stronger for the Ge-rich compounds. For Gd atoms the redistributing affects probably 5*d* electrons, therefore this may explain the magnetic properties variation as the indirect exchange would be based on the interaction via 5*d* electrons more than RKKY-based [39]. The experimental results may be compared with theoretical calcula-

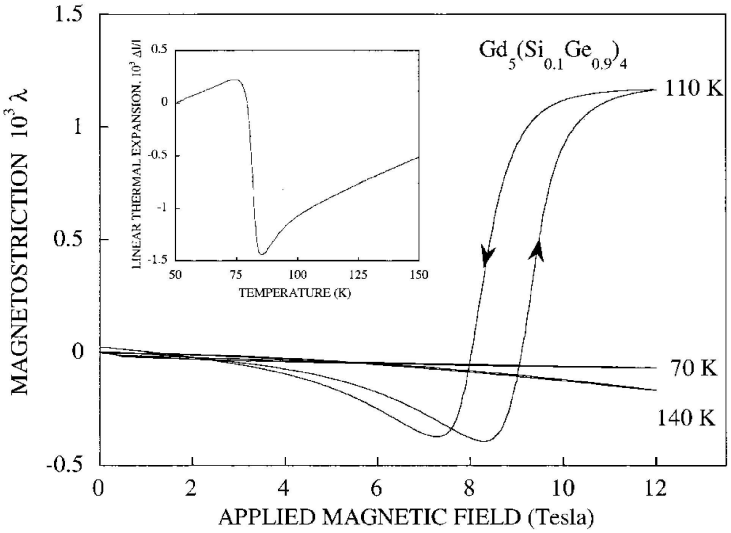

Figure 2.12: Magnetostriction (λ) isotherms along the applied field at some selected temperatures for $Gd_5(Si_xGe_{1-x})_4$ with x=0.1. The inset shows the linear thermal expansion $\Delta l/l$ for increasing temperature along the same measurement direction. Taken from Ref. [9].

tions of the electronic band structure and the density of states [35, 52, 53, 54], which account for the observed resistivity and magnetic behaviour and confirm that the $5d$ character of the valence electrons determines the most important properties of the compounds [52].

2.6.2 Structural characterisation

A large variety of works have studied experimentally the main structural features of $Gd_5(Si_xGe_{1-x})_4$ alloys. To mention some of them: surface structure of single crystals performed with X-ray methods (X-ray powder difraction and Berg-Barret X-ray topography), scanning electron microscopy (SEM) and Auger electron spectroscopy (AES) [55]; observation of the first-order transition with magnetic force microscopy (MFM) [56, 57] and transmission electron microscopy (TEM) [58]; determination of phases in as cast samples using SEM, energy dispersive spectroscopy (EDS) and orientation imaging microscopy [59]; detailed microstructure of monoclinic phase using TEM bright field images and selected area electron diffraction (SAED) [60]; and structural differences between the various phases present in the intermediate-range compounds using TEM [58].

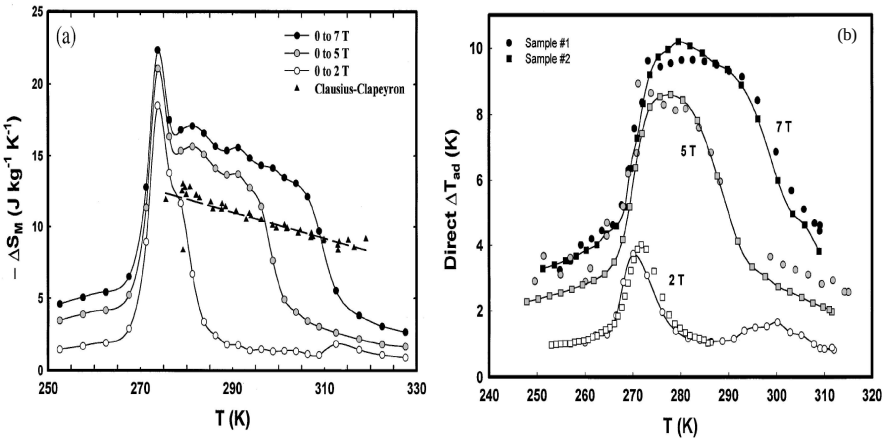

Figure 2.13: (a) Entropy change for increasing fields, as calculated from the Maxwell relation (circles) -with different field variations- and the Clausius-Clapeyron equation (triangles), using magnetisation data for $Gd_5(Si_2Ge_2)$ alloy. (b) Direct measurement of the adiabatic temperature change for two $Gd_5(Si_2Ge_2)$ samples, with different field variations. Taken from Ref. [61].

2.7 Evaluation of the MCE at a first-order transition

The correct evaluation of the entropy change related to the MCE at a first-order transition is a controversial issue and has lately aroused much discussion [4, 61, 62, 63, 64, 65]. For $Gd_5(Si_xGe_{1-x})_4$, Giguère *et al.* [61] showed that the use of the Maxwell relation (Eq. 1.5 and 1.6) to calculate the entropy change overestimates (at least ~20%, see Fig. 2.13 (a)) the value obtained from the Clausius-Clapeyron equation (Eq. 1.17), which the authors [61, 64] claimed to be the correct procedure due to the first-order nature of the transition in these alloys. According to them, the entropy change in the magnetostructural transition is not associated with the continuous change of the magnetisation, M, as a function of T and H, but rather with the discontinuous change in M due to the crystallographic transformation. They claimed that Maxwell relations do not hold since M is not a continuous, derivable function in that case. In contrast, Gschneidner *et al.* [62] argued that the Maxwell relation is applicable even in the occurrence of a first-order transition, except when this transition takes place at a fixed T and H, giving rise to a step-like change of M (*ideal* case). Besides, they claimed that Clausius-Clapeyron equation would imply an H-independent adiabatic temperature change, which however is not consistent

with the experimental observations [61] (see Fig. 2.13 (b)). Moreover, Sun*et al.* [63] showed that the entropy change calculated from the Maxwell relation is indeed equivalent to that given by the Clausius-Clapeyron equation, provided M is considered T-independent in whichever phase the transition involves, and M is a step function with a finite jump at the transition temperature. They also suggested that the two procedures may yield different results since the Clausius-Clapeyron method does not take into account the reduction of spin fluctuations by an applied field.

Furthermore, at a first-order phase transition, the experimental determination of the heat capacity C_P is intrinsically uncertain due to the release of latent heat (*i.e.*, a discontinuity in the entropy), therefore C_P also presents problems in the calculation of the MCE in the vicinity of a first-order phase transition [65]. The entropy discontinuity can be determined from DSC measurements (see sec. 3.2.3 and also Ref. [65]), as it will be shown in Chapter 4. The controversy between the variety of methods to evaluate the MCE at a first-order phase tansition will also be discussed in Chapter 5.

Bibliography

[1] F. Holtzberg, R. J. Gambino, and T. R. McGuire, J. Phys. Chem. Solids**28**, 2283 (1967).

[2] G. S. Smith, A. G. Tharp, and Q. Johnson, Acta Crystallogr.**22**, 940 (1967).

[3] G. S. Smith, Q. Johnson, and A. G. Tharp, Acta Crystallogr.**22**, 269 (1967).

[4] V. K. Pecharsky and K. A. Gschneidner, Jr., Phys. Rev. Lett.**78**, 4494 (1997).

[5] V. K. Pecharsky and K. A. Gschneidner, Jr., Appl. Phys. Lett. **70**, 3299 (1997).

[6] V. K. Pecharsky and K. A. Gschneidner, Jr., J. Alloys Comp.**260**, 98 (1997).

[7] V. K. Pecharsky and K. A. Gschneidner, Jr., J. Magn. Magn. Mater.**167**, L179 (1997).

[8] V. K. Pecharsky and K. A. Gschneidner, Jr., Adv. Cryog. Eng. **43**, 1729 (1998).

[9] L. Morellon, J. Blasco, P. A. Algarabel, and M. R. Ibarra, Phys. Rev. B**62**, 1022 (2000).

[10] L. Morellon, P. A. Algarabel, M. R. Ibarra, J. Blasco, B. García-Landa, Z. Arnold, and F. Albertini, Phys. Rev. B **58**, R14721 (1998).

[11] M. Nazih, A. de Visser, L. Zhang, O. Tegus, and E. Brück, Solid State Comm. **126**, 255 (2003).

[12] P. Schobinger-Papamantellos and A. Niggli, J. Phys. Chem. Solids**42**, 583 (1981).

[13] P. Schobinger-Papamantellos, J. Phys. Chem. Solids**39**, 197 (1978).

[14] C. Ritter, L. Morellon, P. A. Algarabel, C. Magen, and M. R. Ibarra, Phys. Rev. B **65**, 94405 (2002).

[15] C. Magen, Z. Arnold, L. Morellon, Y. Skorokhod, P. A. Algarabel, M. R. Ibarra, and J. Kamarad, Phys. Rev. Lett.**91**, 207202 (2003).

[16] L. Morellon, Z. Arnold, P. A. Algarabel, C. Magen, M. R. Ibarra, and Y. Skorokhod, , to be published.

[17] B. Teng, M. Tu, Y. Chen, and J. Tang, J. Phys.: Condens. Matter **14**, 6501 (2002).

[18] A. O. Pecharsky, V. K. Pecharsky, and K. A. Gschneidner, Jr., J. Appl. Phys. **93**, 4722 (2003).

[19] A. O. Pecharsky, K. A. Gschneidner, Jr., V. K. Pecharsky, and C. E. Schindler, J. Alloys Comp. **338**, 126 (2002).

[20] V. K. Pecharsky, A. O. Pecharsky, and K. A. Gschneidner, Jr., J. Alloys Comp. **344**, 362 (2002).

[21] V. K. Pecharsky, G. D. Samolyuk, V. P. Antropov, A. O. Pecharsky, and K. A. Gschneidner, Jr., J. Solid State Chem. **171**, 57 (2003).

[22] V. K. Pecharsky and K. A. Gschneidner, Jr., Adv. Mater. **13**, 683 (2001).

[23] W. Choe, V. K. Pecharsky, A. O. Pecharsky, K. A. Gschneidner, Jr., V. G. Young, Jr., and G. J. Miller, Phys. Rev. Lett. **84**, 4617 (2000).

[24] E. M. Levin, V. K. Pecharsky, and K. A. Gschneidner, Jr., Phys. Rev. B **62**, R14625 (2000).

[25] G. H. Rao, J. Phys.: Condens. Matter **12**, L93 (2000).

[26] Q. L. Liu, G. H. Rao, H. F. Yang, and J. K. Liang, J. Alloys Comp. **325**, 50 (2001).

[27] R. Zach, M. Guillot, and R. Fruchart, J. Magn. Magn. Mater. **89**, 221 (1990).

[28] H. Wada and Y. Tanabe, Appl. Phys. Lett. **79**, 3302 (2001).

[29] O. Tegus, E. Brück, K. H. J. Buschow, and F. R. de Boer, Nature **415**, 450 (2002).

[30] A. Fujita, Y. Akamatsu, and K. Fukamichi, J. Appl. Phys. **85**, 4756 (1999).

[31] A. Fujita, S. Fujieda, K. Fukamichi, H. Mitamura, and T. Goto, Phys. Rev. B **65**, 14410 (2001).

[32] R. P. Borges, F. Ott, R. M. Thomas, M. Skumrey, J. M. D. Coey, J. I. Arnaudas, and L. Ranno, Phys. Rev. B **60**, 12847 (1999).

[33] E. M. Levin, V. K. Pecharsky, and K. A. Gschneidner, Jr., J. Magn. Magn. Mater. **231**, 135 (2001).

[34] A. Tang, A. O. Pecharsky, D. L. Schlagel, T. A. Lograsso, V. K. Pecharsky, and K. A. Gschneidner, Jr., J. Appl. Phys. **93**, 8298 (2003).

[35] E. M. Levin, V. K. Pecharsky, K. A. Gschneidner, Jr., and G. J. Miller, Phys. Rev. B **64**, 235103 (2001).

[36] E. M. Levin, K. A. Gschneidner, Jr., and V. K. Pecharsky, Phys. Rev. B**65**, 214427 (2002).

[37] C. Magen, L. Morellon, P. A. Algarabel, C. Marquina, and M. R. Ibarra, J. Phys.: Condens. Matter **15**, 2389 (2003).

[38] V. K. Pecharsky, A. P. Holm, K. A. Gschneidner, Jr., and R. Rink, Phys. Rev. Lett. **91**, 197204 (2003).

[39] J. Szade and G. Skorek, J. Magn. Magn. Mater. **196-197**, 699 (1999).

[40] L. Morellon, J. Stankiewicz, B. García-Landa, P. A. Algarabel, and M. R. Ibarra, Appl. Phys. Lett. **73**, 3462 (1998).

[41] E. M. Levin, V. K. Pecharsky, and K. A. Gschneidner, Jr., Phys. Rev. B**60**, 7993 (1999).

[42] E. M. Levin, V. K. Pecharsky, K. A. Gschneidner, Jr., and P. Tomlinson, J. Magn. Magn. Mater. **210**, 181 (2000).

[43] L. Morellon, P. A. Algarabel, C. Magen, and M. R. Ibarra, J. Magn. Magn. Mater. **237**, 181 (2001).

[44] J. Stankiewicz, L. Morellon, P. A. Algarabel, and M. R. Ibarra, Phys. Rev. B **61**, 12651 (2000).

[45] E. M. Levin, V. K. Pecharsky, and K. A. Gschneidner, Jr., Phys. Rev. B**63**, 174110 (2001).

[46] J. B. Sousa, M. E. Braga, F. C. Correia, F. Carpinteiro, L. Morellon, P. A. Algarabel, and M. R. Ibarra, J. Appl. Phys. **91**, 4457 (2002).

[47] E. M. Levin, A. O. Pecharsky, V. K. Pecharsky, and K. A. Gschneidner, Jr., Phys. Rev. B **63**, 064426 (2001).

[48] J. B. Sousa, M. E. Braga, F. C. Correia, F. Carpinteiro, L. Morellon, P. A. Algarabel, and M. R. Ibarra, Phys. Rev. B **67**, 134416 (2003).

[49] M. Han, D. C. Jiles, J. E. Snyder, C. C. H. Lo, J. S. Leib, J. A. Paulsen, and A. O. Pecharsky, J. Appl. Phys. **93**, 8486 (2003).

[50] M. Han, J. A. Paulsen, J. E. Snyder, D. C. Jiles, T. A. Lograsso, and D. L. Schlagel, IEEE Trans. Magn. **38**, 3252 (2002).

[51] M. Han, D. C. Jiles, S. J. Lee, J. E. S. T. A. Lograsso, and D. L. Schlagel, IEEE Trans. Magn. **39**, 3151 (2003).

[52] G. Skorek, J. Deniszczyk, and J. Szade, J. Phys.: Condens. Matter**14**, 7273 (2002).

[53] G. D. Samolyuk and V. P. Antropov, J. Appl. Phys.**91**, 8540 (2002).

[54] B. N. Harmon and V. N. Antonov, J. Appl. Phys.**91**, 9815 (2002).

[55] J. Szade, G. Skorek, and A. Winiarski, J. Cryst. Growth**205**, 289 (1999).

[56] J. Leib, J. E. Snyder, C. C. H. Lo, J. A. Paulsen, P. Xi, and D. C. Jiles, J. Appl. Phys. **91**, 8852 (2002).

[57] J. Leib, C. C. H. Lo, J. E. Snyder, D. C. Jiles, V. K. Pecharsky, D. L. Schlagel, and T. A. Lograsso, IEEE Trans. Magn. **38**, 2441 (2002).

[58] J. S. Meyers, S. Chumbley, F. Laabs, and A. O. Pecharsky, Acta Mater.**51**, 61 (2003).

[59] J. S. Meyers, S. Chumbley, F. Laabs, and A. O. Pecharsky, Scripta Mater. **47**, 509 (2002).

[60] J. S. Meyers, S. Chumbley, W. Choe, and G. J. Miller, Phys. Rev. B **66**, 12106 (2002).

[61] A. Giguère, M. Földeàki, B. Ravi Gopal, R. Chahine, T. K. Bose, A. Frydman, and J. A. Barclay, Phys. Rev. Lett. **83**, 2262 (1999).

[62] K. A. Gschneidner, Jr., V. K. Pecharsky, E. Brück, H. G. M. Duijn, and E. Levin, Phys. Rev. Lett. **85**, 4190 (2000).

[63] J. R. Sun, F. X. Hu, and B. G. Shen, Phys. Rev. Lett. **85**, 4191 (2000).

[64] M. Földeàki, R. Chahine, T. K. Bose, and J. A. Barclay, Phys. Rev. Lett.**85**, 4192 (2000).

[65] V. K. Pecharsky and K. A. Gschneidner, Jr., J. Appl. Phys.**86**, 6315 (1999).